

Experimental Assessment of Passive Capillary Wick Sampler Suitability for Inorganic Soil Solution Constituents

Julia N. Perdrial*

Nicolas Perdrial

Dep. of Soil, Water, and Environ. Sci.
Univ. of Arizona
Tucson, AZ 85720
and

Dep. of Geology
Univ. of Vermont
Burlington, VT 05405

Angelica Vazquez-Ortega

Dep. of Soil, Water, and Environ. Sci.
Univ. of Arizona
Tucson, AZ 85720

Courtney Porter

Dep. of Hydrology and Water Resources
Univ. of Arizona
Tucson, AZ 85720

John Leedy

Jon Chorover

Dep. of Soil, Water, and Environ. Sci.
Univ. of Arizona
Tucson, AZ 85720

Determination of subsurface solute fluxes is central in critical zone (CZ) science because key processes such as bio-geochemical weathering, nutrient dynamics, and contaminant transport can be determined. With passive capillary fiberglass wick samplers (PCaps), solute, and water fluxes can be assessed; however, the presence of fiberglass can impact soil solution chemistry. To determine which solutes are suitable for sampling by fiberglass wick PCaps, flow-through experiments were performed where aqueous soil extracts were percolated through the wicks and changes in effluent solution pH, dissolved inorganic carbon (DIC), anions, major cations, and trace metals including rare earth elements (REE) were monitored. Results indicated dissolution of wicks releasing the glass constituents B, Na, Si, Ca, Mg as well as F⁻ and DIC. Barium, K, and Sr were retained, likely due to exchange reactions with either glass constituents or interlayer cations of clay colloids. Stop-flow was included to mimic precipitation events revealing increased pulse-like release of glass constituents. Results of the full-scale experiment indicate substantial contribution from wick material (59 ± 20 for Si, 92 ± 7 for Na, 29 ± 19 for Mg, and -26 ± 32 for Ca, all values in percentage of total effluent concentrations) that cannot be corrected for, hence the use of PCaps for these solutes is not recommended. A great number of other solutes were however not impacted by the presence of wicks such as most anions (Cl⁻, NO₃⁻, SO₄²⁻) and many trace metals (Al, Ti, Mn, V, Fe, Co, As, Y, Mo, Sn, Pb, U, and all REE).

Abbreviations: ASE, aqueous soil extracts; CZ, critical zone; DIC, dissolved inorganic carbon; DOM, dissolved organic matter; HDPE, high density polyethylene; IC, inorganic carbon; ICP-MS, inductively coupled plasma mass spectrometry; JRB-SCM CZO, Jemez River Basin-Santa Catalina Mountains Critical Zone Observatory; LOD, limit of detection; PCaps, passive capillary fiberglass wick samplers; PV, pore volume; REE, rare earth elements; SHM, Stockholm Humic Model; TOC, total organic carbon; ZOB, zero-order basin; ZTS, zero-tension pan samplers.

Accurate determination of subsurface solute fluxes is central in CZ science because they are needed to quantify key processes such as (i) mineral weathering and chemical denudation, (ii) CZ biogeochemical cycling and nutrient dynamics, and (iii) transport or retention of contaminants. For example, solute fluxes derived from silicate weathering are used to quantify the CZ's capacity to neutralize acids, for example, from acid rain but also the extent of CO₂ consumption during silicate hydrolysis, a process particularly important with respect to the coupling of increased atmospheric CO₂ levels and global climate change

Soil Sci. Soc. Am. J. 78:486–495

doi:10.2136/sssaj2013.07.0279

Received 13 Sept. 2013.

*Corresponding author (Julia.Perdrial@uvm.edu).

© Soil Science Society of America, 5585 Guilford Rd., Madison WI 53711 USA

All rights reserved. No part of this periodical may be reproduced or transmitted in any form or by any means, electronic or mechanical, including photocopying, recording, or any information storage and retrieval system, without permission in writing from the publisher. Permission for printing and for reprinting the material contained herein has been obtained by the publisher.

(Amiotte Suchet et al., 2003). Determination of soluble nutrient fluxes can help to determine ecosystem nutrient cycling dynamics and/or impacts of agricultural production (Barber, 1995). Similarly, there is a strong need for methods that enable in situ monitoring of contaminant metal (e.g., Pb) and/or radionuclide (e.g., U) fluxes in the vadose zone (Boulding and Ginn, 2004).

A number of techniques have been proposed to determine subsurface solute composition and fluxes (Weihermüller et al., 2007), but to utilize them it is necessary to know solute concentration, sampled volume, and contributing area. These requirements are met for zero-tension pan “lysimeters” that sample gravitational water during saturated conditions as well as for PCaps, that are suitable for use under both saturated and unsaturated conditions (Brandi-Dohrn et al., 1996; Jabro et al., 2008; Louie et al., 2000; Zhu et al., 2002). Because of the predominance of unsaturated flow in soils, PCaps are widely employed at the Jemez River Basin–Santa Catalina Mountains Critical Zone Observatory (JRB-SCM CZO; Chorover et al., 2011).

The sampling principle of PCaps is the generation of a hanging water column that exerts a tension on the soil–wick interface whose magnitude is directly proportional to the vertical length of the wick material (Biddle et al., 1995; Frisbee et al., 2010; Holder et al., 1991). Solution held in the soil at potential values higher than that imposed by the device are collected, however when the gradient imposed by the sampler is higher than the soil matric potential, soil solution collection will stop. Therefore, PCaps are not ideal for sampling under fairly dry soil conditions where the necessary gradient cannot be established. Another caveat of PCaps (and virtually all in situ soil solution sampling devices) is the introduction of artifacts during installation, such as creation of preferential flow paths (Mertens et al., 2007; Miro et al., 2010; Perdrial et al., 2012; Peters and Durner, 2009). In this case, sampled soil solution is not likely to be representative of bulk soil solution. Taking these limitations into consideration, solute fluxes can be readily calculated if both sample volume and solute concentration of the soil solution draining into the collection vessel are known.

However, the requisite contact of the water column with fiberglass wick material during transport into a sampling vessel may alter the composition of the sample, motivating correction for wick interaction following sample geochemical analysis (Goyne et al., 2000). Studies have addressed this effect showing, for example, that certain mineral colloids (e.g., ferrihydrite, feldspathoids, montmorillonite, and kaolinite) can be retained at the wick–water interface (Czigány et al., 2005; Ilg et al., 2007; Shira et al., 2006). Dissolved inorganic carbon concentration and alkalinity determined on PCap samples were higher than in co-located zero tension pan samplers (ZTS), an effect that was attributed to trace dissolution of the wick material, but with results also likely affected by differential sampling of macro-pore (higher with ZTS) versus matrix (higher with PCaps) soil waters (Goyne et al., 2000). Changes in pH affected solute speciation, especially for DIC and Al, whereas other solutes (e.g., some

anions, Fe and Mn) were not significantly affected by transport along the glass wick surface.

In a recent study on dissolved organic matter (DOM), wicks were shown to not detectably sorb, release, or fractionate DOM that was sampled both in laboratory experiments and CZ field sites (Perdrial et al., 2012). Notwithstanding soil physical effects, such as introduction of preferential flow or local alteration of the flow domain—common to in situ sampling technologies in general—it was concluded that PCaps effectively sample representative DOM in mobile soil solutions of the JRB-SCM CZO (Perdrial et al., 2012). That study highlighted the utility of combining laboratory experiments (with natural soil solutions) and field-based soil solution collections to evaluate quantitatively the behavior of PCaps in the unsaturated zone.

Despite important prior research on PCap utility for soil solution sampling, suitability for a number of solutes relevant to CZ weathering processes, including DIC, major cations and anions, and trace metal(loid)s (including potential contaminants and REE) remains unclear. In this work, therefore, we report results of experiments designed to measure the reaction of rock-weathering derived solutes with wick material. We employ an experimental design similar to that used by Perdrial et al. (2012) to determine which solutes move conservatively versus non-conservatively through the wicks, and to determine whether predictive accounting can be developed for non-conservative solutes that enable quantitative corrections to field solutions collected in the field for subsequent instrumental geochemical analysis.

EXPERIMENTAL AND FIELD METHODS

Experimental Design and Wick Preparation

Fiberglass wick material was obtained from Pepperell and Braiding Co. (#1381, Pepperell, MA) and pretreated according to the procedure described in Goyne et al. (2000) and Knutson et al. (1993). Briefly, wicks (9.5 mm in diam.) were cut to 10 cm length, combusted at 400°C for 4 h to remove organics, then washed with phosphate-free dilute detergent and rinsed several times with ultrapure (18.2 MΩ·cm) water. Material was then washed twice in 10 mM HCl followed by daily rinses with ultrapure water for 4 wk.

Wick Column Experiment

To obtain high time resolution datasets on wick solute uptake and release, cleaned wicks, saturated with ultrapure water, were mounted in triplicate into acid-washed and combusted glass columns of 14 cm length and 1.5 cm diameter. Ashless Whatman 41 filters introduced at the column outlet prevented particles >20 μm from leaving the columns. Influent solutions (experimental soil solution or ultrapure water, detailed below) were continuously stirred and delivered to the wick surface drop wise at a constant rate of 0.6 mL min⁻¹ through acid washed polytetrafluoroethylene tubing to simulate unsaturated vertical flow in the vadose zone and to reproduce realistic wick flow velocities. Effluent solutions were collected into acid-washed, combusted glass vials with an ISCO Foxy 200 fraction collector (ISCO Co., Lincoln, NE) every 12.4 mL

(corresponding to about 2 pore volumes [PV], Fig. 1a). Repeat infiltration events were simulated by interrupting each of three infiltration cycles of 3.5 h with a 24-h stop-flow period during which the experimental wicks were not allowed to dry completely but were drained gravitationally. The daily sampled influent and effluent solutions were analyzed for all target constituents to enable direct quantification of wick contact effects. The full ranges of chemical parameter concentrations are indicated in the results section.

A separate set of wicks were run for one infiltration cycle specifically to obtain in-line pH measurements in real time using a gel-filled electrode (VWR symphony, Radnor, PA). Electrode calibration was performed at the beginning and end of the experiment and a linear correction to calibration was applied when needed. Effluent pH was recorded over a single flow-through cycle (without stop flow) every 2 min and averaged every three measurements (corresponding to ~ 1 PV). For the infiltrating solutions, pH values were recorded at the start and the end of each infiltration period.

Full Scale Experiment on Passive Capillary Fiberglass Wick Samplers

A full scale experiment using fully constructed PCaps (designed as described in Perdrial et al., 2012) was additionally performed to complement the column experiment and to provide data for the field-deployable scale. Briefly, each PCap consists of a 30.5 by 30.5 cm acid washed high density polyethylene (HDPE) sheet of 1.9 cm thickness with a 5.1-cm hole in the center that accommodates a polypropylene elbow fitting. Nylon strips fixed on the HDPE sheet hold the wicks in place with a novel construction that avoids the use of manufactured adhesives that could affect biogeochemical measurements. A 45-cm polyvinyl chloride (PVC) tube is inserted under the sheet and guides the wicks to the collection vessel. Three PCap replicates each containing 10 clean wicks of a 9.5-mm diam. and a 60-cm length were installed in the laboratory (Fig. 1b). Influent solution was supplied at (i) a constant rate of 0.8 mL min^{-1} to simulate diffusive flow dynamics and (ii) by flushing the solution through the material to simulate fast, macropore flow ($\sim 1000 \text{ mL min}^{-1}$). Three stop flow events, each of a 5-d duration, were included where the wicks were allowed to dry before flow was reapplied. It is worth considering that in this experiment, the PCaps were dried down during these stop flows to equilibrium with relative humidities that are much lower than anticipated to occur in natural soils.

Infiltration Solution

Aqueous soil extracts (ASE) of a B-horizon soil were used as influent solutions. The soil was pre-sampled from a planar hillslope location in

the mixed conifer zero order basin (ZOB) site of JRB-SCMCZO (“pedon1”) and classified as a fine-loamy, mixed, superactive Oxyaquic Haplocryoll (Soil Survey Staff, 2010). Quantitative X-ray diffraction revealed a mineralogy dominated by quartz (38%), muscovite (32%), orthoclase (12%), albite (7%), and kaolinite (5%). The soil contained 30 mg inorganic carbon (IC) and 3050 mg total organic carbon (TOC) per kilogram of soil. To obtain ASE, sieved (<2 mm) field moist B horizon soil was added to three 1000 mL HDPE bottles and the dry mass of the soil was calculated based on soil moisture content determined on subsamples (~25% water content). Ultrapure water added was equivalent to the mass of dry soil (~500 g) minus the water already contained in the soil ($500 \text{ g} - 125 \text{ g} = 375 \text{ g}$), yielding a soil/water mass ratios of 1:1. Bottles were tightly capped and shaken at 180 rpm for 24 h, where after suspensions were centrifuged ($7000 \times g$ for 30 min), supernatant solutions were filtered (0.45- μm Nylon membranes) and combined into one 2.5-L glass bottle.

Chemical Analysis

Dissolved inorganic and organic C was determined by acidification followed by infrared and chemiluminescence gas detection (DIC), as well as catalytic oxidation at 720°C (dissolved organic C), using a Shimadzu TOC-VCSH (Shimadzu Scientific Instruments, Columbia, MD). Inorganic anions (Cl^- , F^- , NO_2^- , NO_3^- , SO_4^{2-} , PO_4^{3-}) were measured by ion chromatography (Dionex Ion Chromatograph DX-500, Sunnyvale, CA) using the Ion Pac AS11 column with a guard column (AG11) and sodium hydroxide (50 mM) as the mobile phase. Metals and metal(loid)s were measured following sample acidification and appropriate dilution before inductively

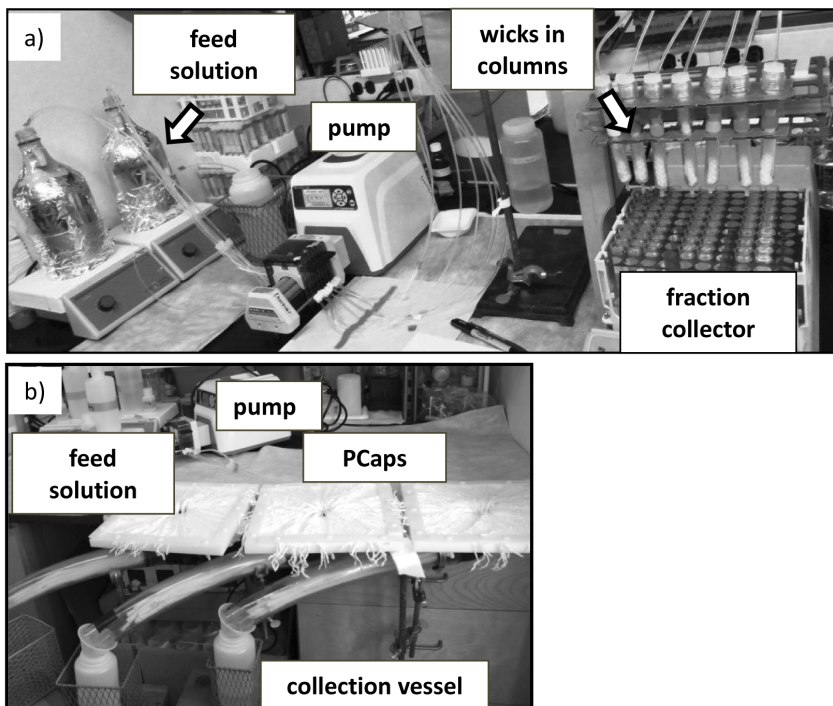


Fig. 1. Experimental design for testing mechanisms of wick-solution interaction (a) at the column scale and (b) at the full field-deployable scale.

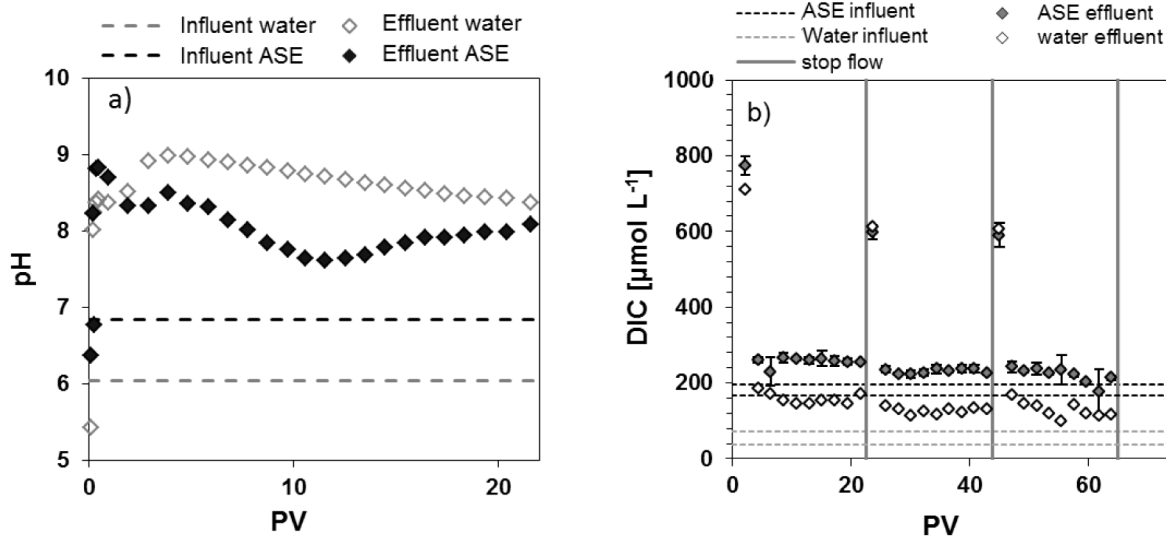


Fig. 2. (a) Evolution of pH during the first infiltration cycle for aqueous soil extract and water blank. (b) Influent and effluent values dissolved inorganic carbon (DIC) for all three infiltration cycles. Range of influent solution concentrations are indicated by dotted horizontal lines and vertical lines indicate 24 h of stop flow.

coupled plasma mass spectrometry (ICP-MS, ELAN DRC-II, PerkinElmer, Shelton CT).

Soil solution speciation was calculated using MINTEQ3.0 (EPA 2006) where all major solution constituent concentrations as well as pH were included. Assessment of metal-humic complexation was included using the Stockholm Humic Model (SHM; Gustafsson, 2001) included in MINTEQ3.0. For calculations, humic substances were assumed to have fulvic acid character and DOM/DOC ratio was set to 1.65 based on ongoing Critical Zone Observatory (CZO) measurements (Perdrial et al., 2012).

RESULTS

Column Experiments pH and Dissolved Carbon

For both ASE solutions and pure water controls, the first effluent pH measurement (0.1 PV) was lower than influent solution (5.4 in effluent vs. 6.0 in influent for water and 6.3 in effluent vs. 6.8 in influent for ASE) but thereafter values increased rapidly to significantly higher than influent indicating proton consumption (Fig. 2a). For water, effluent pH reached a maximum of 9 at PV 4 before decreasing steadily to 8.1 after 22 PV. A more complex behavior was observed for ASE solution; after quickly reaching a maximum pH value of 8.8 (at 0.4 PV) pH dropped to 8.3 (2–3 PV), increased slightly to 8.5 (4 PV), and then consistently approached a second pH minimum of 7.6 (11 PV), thereafter increasing steadily to a value of 8.1 at 22 PV. Note that no stop flow could be included in these in-line pH measurements and only the first infiltration cycle is shown.

Effluent DIC concentrations were mostly above influent DIC concentrations (Fig. 2b, 61 ± 15 and $178 \pm 13 \mu\text{mol L}^{-1}$ for water and ASE, respectively). Highest ASE effluent concentrations were observed in the first PV's after (re)-application of flow (770 , 600 , and $590 \mu\text{mol L}^{-1}$ for 2, 24, and 45 PV, respectively),

whereas all other PV's averaged at much lower values ($240 \pm 25 \mu\text{mol L}^{-1}$). Water control effluent followed the same general trend with highest concentrations in the first PV's after (re)-application of flow.

Inorganic Anions

Fluoride was below detection (limit of detection [LOD] $< 2 \mu\text{mol L}^{-1}$) in the ASE (Fig. 3a) and in the water influent but was quantifiable in ASE effluent solutions, with highest concentrations in the first PV's after (re)-application of flow (up to $29.5 \pm 10.3 \mu\text{mol L}^{-1}$). Thereafter, F⁻ ASE effluent concentrations averaged $2.2 \pm 3.9 \mu\text{mol L}^{-1}$. Fluoride was the only anion that was detected in the water effluent (all other anions were below detection with LOD $< 4 \mu\text{mol L}^{-1}$ and are therefore only described for ASE) and spiked in the PV's after (re)-application of flow (25.8 , 10.4 , and $8.7 \mu\text{mol L}^{-1}$). Chloride concentrations in ASE influent ranged from 20 to $22 \mu\text{mol L}^{-1}$. Chloride effluent values were low in first sample (2 PV, Fig. 3b), likely due to dilution by water present in the wicks. Values fluctuated during the first two infiltration cycles and stabilized at effluent values ($22.1 \pm 2.8 \mu\text{mol L}^{-1}$) statistically equivalent to influent concentrations. Nitrate concentration in ASE influent ranged from below detection to $5.18 \mu\text{mol L}^{-1}$. This variation was likely due to microbial processing during stop flow and caused ASE effluent solution values to be variable as well (ranging from $11 \pm 3.6 \mu\text{mol L}^{-1}$ at 4 PV to below detection). Aqueous soil extracts influent SO_4^{2-} concentration showed a more narrow range (11.4 – $12.7 \mu\text{mol L}^{-1}$), and ASE effluent concentrations remained mostly within the range of influent solution during the first infiltration cycle, with greater variation during the second and third cycles (Fig. 3d). Resulting average effluent concentrations for the entire experiment were $11 \pm 3.5 \mu\text{mol L}^{-1}$.

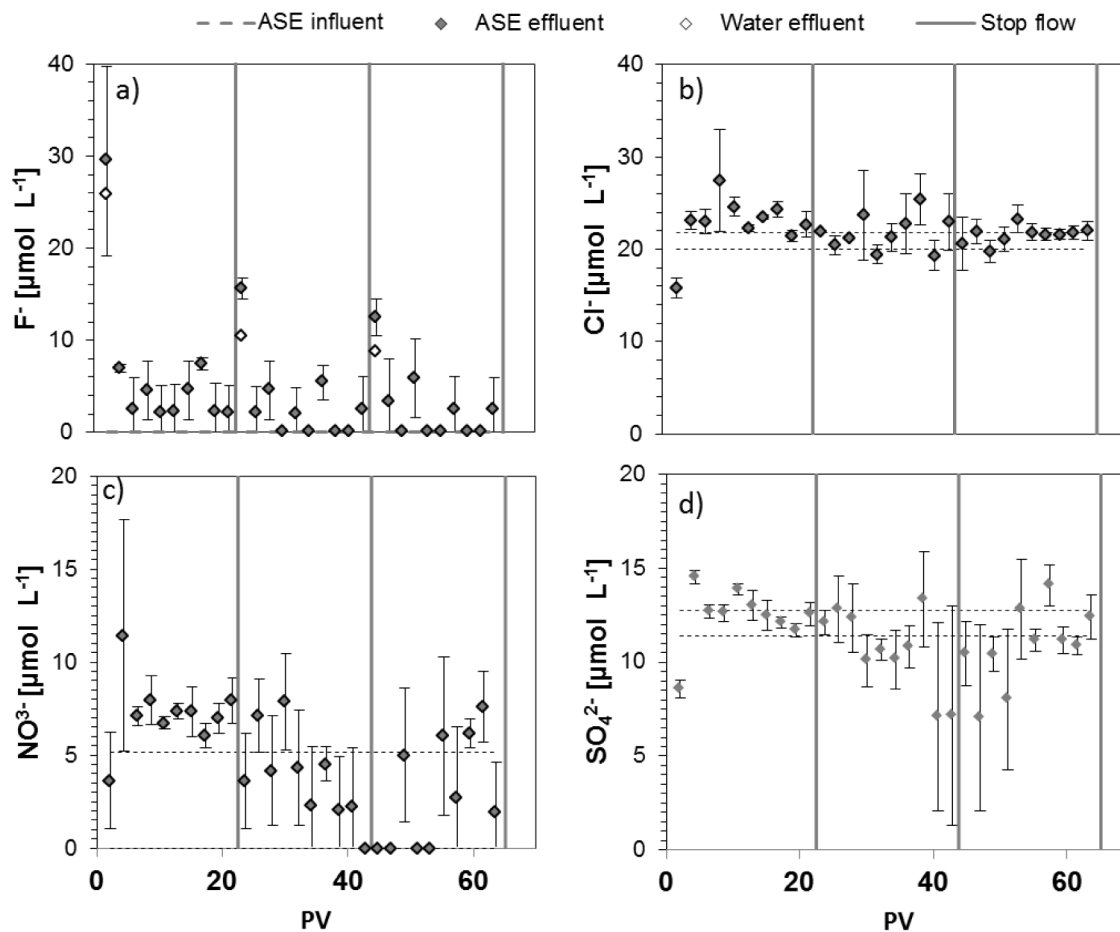


Fig. 3. Influent and effluent values for (a) F^- , (b) Cl^- , (c) NO_3^- and (d) SO_4^{2-} for aqueous soil extract (ASE) as well as water. Range of Influent solution concentrations are indicated by dotted horizontal lines. Vertical lines indicate 24 h of stop flow.

Major Cations and Trace Elements

Sodium ASE and water effluent solution concentrations exceeded those of influent solutions ($<1 \mu\text{mol L}^{-1}$ for water and $24.7 \pm 0.1 \mu\text{mol L}^{-1}$ for ASE), especially at early reaction times and most significantly just after (re)-application of flow (Fig. 4a). Aqueous soil extracts effluent Na concentrations in the first PV after application was highest ($236 \mu\text{mol L}^{-1}$) and decreased for the second and third pulse ($93.1 \mu\text{mol L}^{-1}$ at PV 24 and $74.1 \mu\text{mol L}^{-1}$ at PV 45). Aside from the spikes, average ASE effluent Na concentrations ($40 \pm 14 \mu\text{mol L}^{-1}$) were slightly higher than influent concentrations. Water effluent Na concentration showed a similar behavior, spiking after (re)-application of flow to 214, 63, and $34 \mu\text{mol}$, respectively.

Like it was the case for Na, Si influent concentrations for water ($6.1 \pm 0.1 \mu\text{mol L}^{-1}$) and ASE ($514 \pm 9 \mu\text{mol L}^{-1}$) were lower than Si effluent concentrations (Fig. 4b). Especially after (re)-application of flow, effluent concentrations spiked to values between 531 and $708 \mu\text{mol L}^{-1}$ for water and 939 and $987 \mu\text{mol L}^{-1}$ for ASE and concentrations remained elevated thereafter ($640 \pm 40 \mu\text{mol L}^{-1}$ for ASE and $114 \pm 34 \mu\text{mol L}^{-1}$ for water). Other cations and trace metals that showed pulse-like concentration increases and effluent concentrations that exceeded influent concentrations were B, Mg, Ca, Cr, and Sb (Table 1).

Both K and Sr exemplify behavior of elements for which influent ASE concentration was higher than ASE effluent concentration (Fig. 4c and d), indicating net retention while the first PV after (re)-application of flow showed higher values than the following solutions. For K, lowest ASE effluent concentrations (e.g., $19.1 \pm 0.6 \mu\text{mol L}^{-1}$) were limited to the first infiltration cycle, where effluent concentrations were approximately three times lower than influent ($67.8 \pm 0.1 \mu\text{mol L}^{-1}$). During the second and third infiltration cycles, ASE effluent K concentrations exceeded influent concentrations right after (re)-application of flow. Potassium in pure water influent was below detection ($\text{LOD} < 0.003 \mu\text{mol L}^{-1}$), hence effluent was always above influent water concentrations.

In the case of Sr, ASE effluent concentrations (averaging at $0.10 \pm 0.03 \mu\text{mol L}^{-1}$) remained below influent concentrations ($0.49 \pm 0.00 \mu\text{mol L}^{-1}$) for the entire duration of the experiment. Strontium concentrations in water influent and effluent were always below detection ($\text{LOD} < 0.001 \mu\text{mol L}^{-1}$). Similar behaviors, indicating removal from solution to the wick surfaces, were observed for Ba and Cu (Table 1).

Aluminum and Mn are example elements for which ASE effluent concentrations matched influent concentrations more closely (Fig. 4e and 4f). Although ASE Al effluent concentrations showed large variations during the first

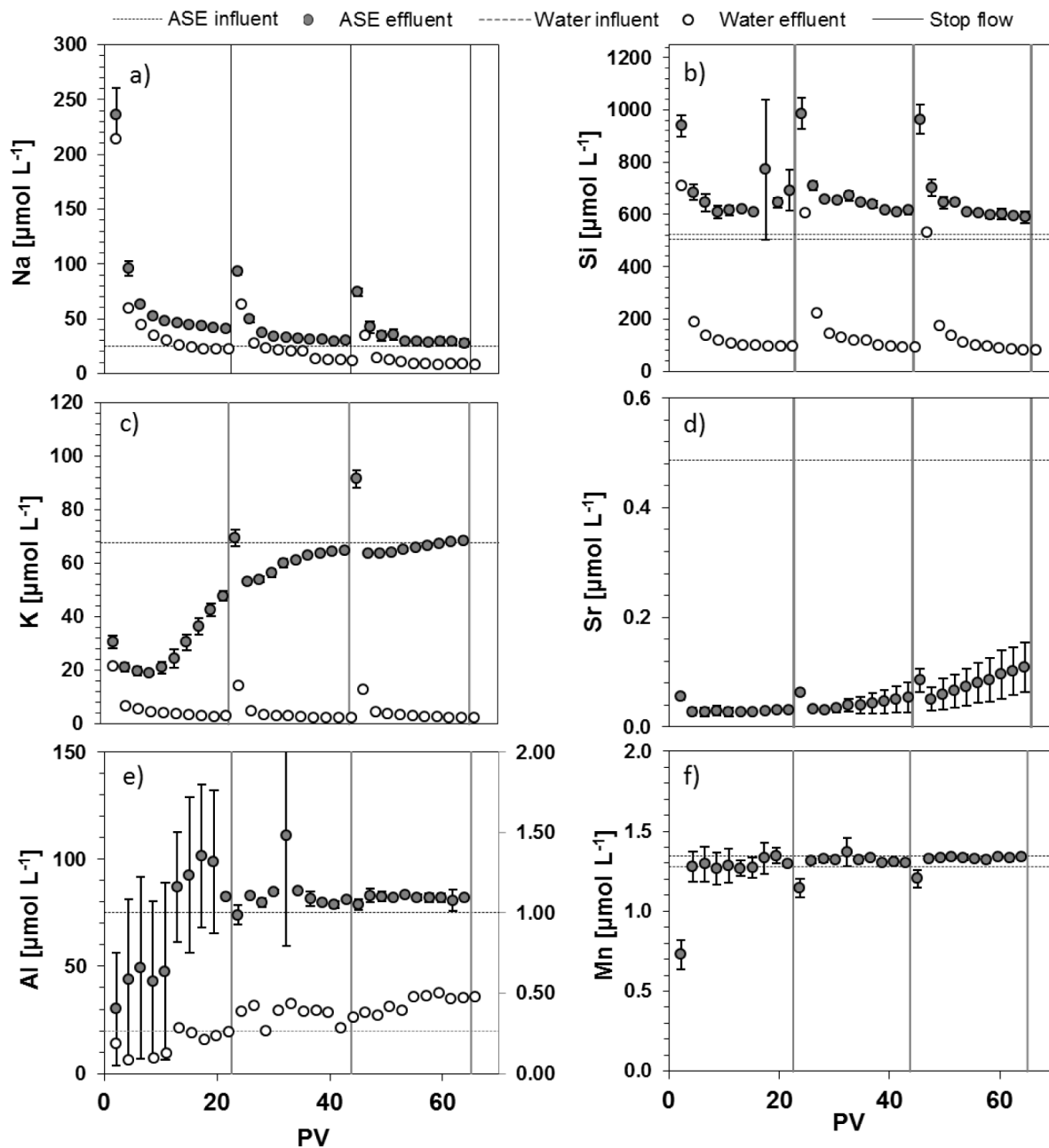


Fig. 4. Influent and effluent values for (a) Na, (b) Si, (c) K, (d) Sr, (e) Al, and (f) Mn for aqueous soil extract (ASE) as well as water. Range of influent solution concentrations are indicated by dotted horizontal lines. Vertical lines indicate 24 h of stop flow.

infiltration cycle, they stabilized during the following two cycles at $83 \pm 7 \mu\text{mol L}^{-1}$, a value that was <10% higher than ASE influent solution ($75 \pm 0.2 \mu\text{mol L}^{-1}$). Pure water Al effluent solutions fluctuated and exceeded influent water concentration ($0.27 \pm 0.01 \mu\text{mol L}^{-1}$) for most of the second and third infiltration cycle (average $0.40 \pm 0.06 \mu\text{mol L}^{-1}$). Other elements that also stabilized after initial fluctuations were Ti, V, As, Mo, Sn, and U (Table 1). Element effluent concentrations exceed influent concentrations by <4% for Sn, V, and U, and by <10% for Mo, but show larger differences for Ti and As (~30%).

Average Mn effluent concentration ($1.31 \pm 0.03 \mu\text{mol L}^{-1}$) was likewise close to average influent solution concentration ($1.31 \pm 0.03 \mu\text{mol L}^{-1}$), however in this case distinct negative pulses with lower effluent concentrations after each

(re)-application of flow was observed (Fig. 4f). Manganese concentrations in water influent and effluent were below detection ($\text{LOD} < 0.002 \mu\text{mol L}^{-1}$). Similar behaviors (negative pulse at [re]-application) were observed for Fe, Co, and Pb where after respective effluent concentrations were close to influent solution concentration (Table 1).

Rare Earth Elements and Yttrium

All rare earth elements (REE) and Y water influent and effluent concentration were below detection ($\text{LOD} < 0.007 \text{ nmol L}^{-1}$), therefore only concentration for ASE solution are described. The pattern for La is exemplary for most REE (including Ce, Pr, Nd, Sm, Gd, Tb, Dy, Ho, Er, Yb) and Y, showing relatively low variation and slightly higher effluent

versus influent concentrations for the first two infiltration cycles that then match the range of influent concentrations during the third infiltration cycle (Fig. 5a). Averaging over the entire experimental duration, effluent concentrations exceeded influent concentrations by <8% for La to Sm (most of the light REE) and by >11% for Gd to Lu (most of the heavy REE, Table 2). Europium effluent was fairly consistent throughout the experiment, remaining lower than influent solution (on average 13% lower, Fig. 5b, Table 2). Similar results were obtained for Lu with mean effluent concentration values ($0.09 \pm 0.02 \mu\text{mol L}^{-1}$) remaining close to those of influent solutions ($0.09 \pm 0.01 \mu\text{mol L}^{-1}$), mean deviations between them being about 1% (Fig. 5c). Likewise, Tm had equal mean concentrations in effluent and influent solutions (Table 2).

Solute Speciation and Charge Balance

Solute speciation for ASE, calculated using MINTEQA3.0, showed that most solutes in ASE influent solution were present as free (aquo) cations and anions (Na^+ , Mg^{2+} , K^+ , Ca^{2+} , F^- , Cl^- , NO_3^- , SO_4^{2-}). Calcium, Mg, and Al were also present in ASE influent solution as charge-neutral DOM-metal complexes, but at the experimental pH most Al was present as $\text{Al}(\text{OH})_4^-$ (60%) and $\text{Al}(\text{OH})_3^0$ (17%, Table 3). Influent ASE Si was present as H_4SiO_4 , and dominant DIC species were HCO_3^- (76%) and H_2CO_3 . Aqueous soil extracts effluent speciation was similar to influent for most solutes (Na^+ , H_4SiO_4 , K^+ , F^- , Cl^- , NO_3^- , SO_4^{2-}). The fraction of Ca and Mg complexed with DOM in ASE effluent decreased after [re]-application of flow and increased thereafter by ~10%. Most Al in the effluent was present as $\text{Al}(\text{OH})_4^-$ (98% after [re]-application of flow and ~95% thereafter) and the dominant DIC species was HCO_3^- (97%) in all PV effluents (Table 3).

Speciation results were used to calculate the charge balance for influent and effluent as a function of PV. The DOM contributed as monovalent negative charge (~50%

Table 1. Average ASE influent and effluent concentration for cations and trace metals. Cumulative element release (positive values) and retention (negative values, underlined) are calculated by subtracting volume weighted average of effluent from influent. Effluent pulses are spiking solute concentrations in the first PV after (re)-application of flow and are reported separately from effluent (all pore volumes except pulses):

	Influent		Effluent pulse (PV 2, 24, 45)		Effluent (except PV 2, 24, 45)		cumulative release or retention	
	[$\mu\text{mol L}^{-1}$]		[$\mu\text{mol L}^{-1}$]		[$\mu\text{mol L}^{-1}$]		μM	
	Average	Stdv.	Average	Stdv.	Average	Stdv.	Average	Stdv.
B	3.1	0.2	41	28	4.4	1.0	1930	180
Na	24.8	0.4	134	72	40	14	9600	370
Mg	63	0.2	186	19	103	16	19490	40
Al	75	0.2	61	22	80	16	1120	20
Si	517	6	963	19	641	42	62120	340
P	1	1.2	1.0	0.9	1.5	0.9	350	20
K	68	0.1	64	25	52	17	<u>-5920</u>	60
Ca	31	0.0	162	14	41	7	8760	30
Ti	0.87	0.15	1.02	0.23	1.19	0.42	120	10
Mn	1.31	0.03	1.03	0.21	1.32	0.03	<u>-10</u>	3
V	0.16	0.01	0.13	0.04	0.15	0.02	<u>-2</u>	0.3
Cr	0.02	0.002	0.08	0.00	0.03	0.00	5	2
Fe	31	1	26	6	31	3	<u>-45</u>	20
Co	0.02	0.00	0.02	0.00	0.02	0.001	0	0.3
Cu	0.19	0.002	0.08	0.01	0.12	0.002	<u>-29</u>	0
As	0.01	0.0004	0.01	0.00	0.01	0.002	1	0.02
Sr	0.49	0.003	0.07	0.01	0.05	0.02	<u>-174</u>	0
Mo	0.001	0.0001	0.001	0.001	0.002	0.001	0	0
Ba	1.84	0.004	0.05	0.01	0.06	0.004	<u>-700</u>	20
Pb	0.02	0.001	0.01	0.00	0.02	0.0004	0	10
U	1.29	0.016	1.21	0.09	1.33	0.10	15	10

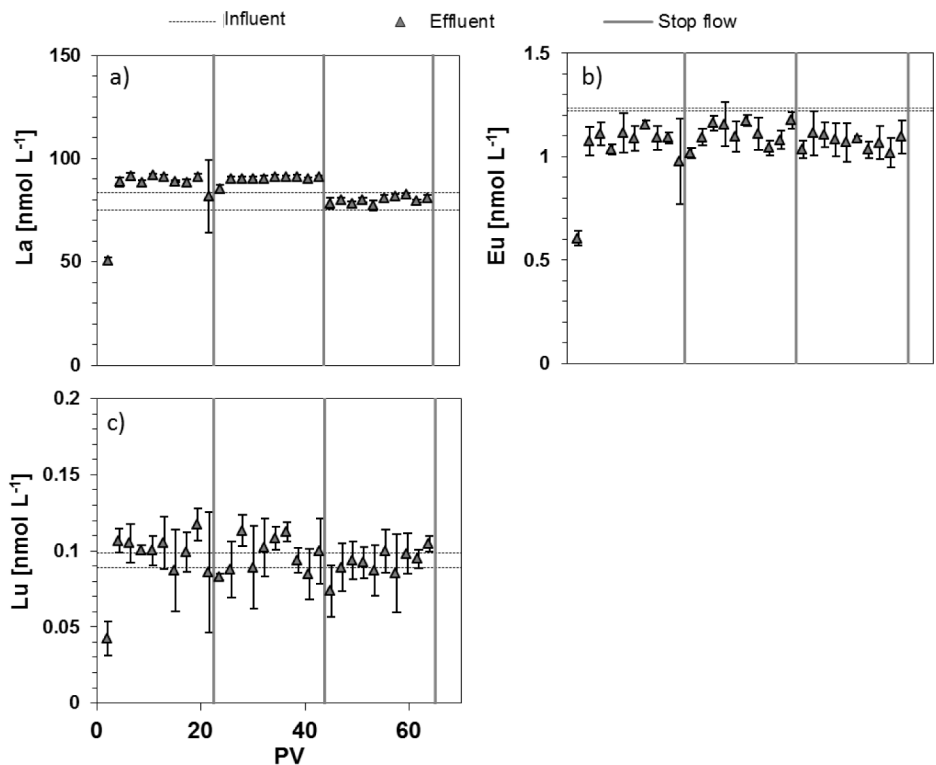


Fig. 5. Influent and effluent values for (a) La, (b) Eu, and (c) Lu for aqueous soil extract (ASE). Range of influent solution concentrations are indicated by dotted horizontal lines. Vertical lines indicate 24 h of stop flow.

Table 2. Average aqueous soil extracts (ASE) influent and effluent concentration for rare earth elements (REE). Cumulative element release are calculated by subtracting volume weighted average of effluent from influent. Effluent pulses are spiking solute concentrations in the first PV after (re)-application of flow and are reported separately from effluent (all pore volumes except pulses):

	Influent		Effluent pulse (PV 2, 24, 45)		Effluent (all except PV 2, 24, 45)		cumulative release	
	[$\mu\text{mol L}^{-1}$] average	stdv.	[$\mu\text{mol L}^{-1}$] average	stdv.	[$\mu\text{mol L}^{-1}$] average	stdv.	[μmol] average	stdv.
Y	33.2	1.6	28.5	5.7	36.2	2.0	910	20
Ce	180.5	10.0	162.6	32.0	197.8	10.6	5500	90
Pr	17.3	1.1	15.8	3.2	19.3	1.1	660	9
Nd	62.1	4.4	56.2	11.6	68.7	4.1	2140	40
Sm	10.5	0.8	9.3	2.0	11.4	0.7	270	10
Gd	8.77	0.38	8.13	1.74	9.90	0.66	380	7
Tb	1.11	0.08	0.98	0.20	1.22	0.08	36	1
Dy	4.79	0.09	4.25	0.87	5.39	0.34	190	4
Ho	0.73	0.05	0.67	0.14	0.82	0.05	30	1
Er	1.80	0.12	1.67	0.30	2.03	0.11	74	2
Tm	0.19	0.01	0.15	0.04	0.19	0.01	1.2	0.3
Yb	0.95	0.04	0.86	0.15	1.09	0.07	46	2

for the influent and 65% for the effluents). The impact of the wicks on the charge balance of ASE solution is summarized in the charge balance diagram (Fig. 6). Positive charges were dominated by the presence of Mg, Ca, and Na and negative charges by DIC, DOC, and Al. Spikes of positive charges were counteracted by DIC only.

Full Scale Experiment

The full scale experiment was included to determine whether the contribution of Si, Na, Ca, and Mg from the wicks can be corrected for in field scale measurements. Effluent concentrations for Si, Na and Mg exceeded influent concentrations throughout the experiment (see supplementary figure). In the case of Si and Na, effluent concentrations were highest during the first three

Table 3. MINTEQ3.0 speciation results for ASE influent and effluent solution in percent of total analyzed concentration for Al and dissolved inorganic carbon. 2PV represents speciation after application of flow and 21 PV during quasi steady-state conditions:

Species	Feed	Effluent pulse (2PV)	Effluent steady state (21PV)
AlOH ⁺ ₂	0.2	/	/
Al(OH) ²⁺	6.1	< 0.1	< 0.1
Al(OH) _{3(aq)}	16.8	0.9	1.9
Al(OH) ⁴⁻	59.8	97.7	94.9
Al ₂ (OH) ₂ CO ₃ ⁺²	0.4	/	/
/FA ₂ AlOH _(aq)	15.8	1.3	3.2
/FA ₂ Al ⁺ _(aq)	0.8	/	< 0.1
CO ₃ ⁻²	< 0.1	1.1	0.5
HCO ₃ ⁻	76.2	97.3	97.2
H ₂ CO ₃ [*] _(aq)	23.7	1.0	2.1
MgCO _{3(aq)}	/	0.1	< 0.1
MgHCO ₃ ⁺	< 0.1	0.2	0.1
CaHCO ₃ ⁺	< 0.1	0.2	< 0.1
CaCO _{3(aq)}	/	0.2	< 0.1

infiltration steps, whereas for Mg effluent concentrations increased over the course of the experiment. Conversely, Ca effluent concentrations were generally lower than those of influent solutions. No effect of infiltration dynamics (slow infiltration vs. flushing) on solute release was apparent, although drying steps diminished Si release immediately after (re)-application of flow, and Si concentrations increased once the wicks were wetted.

The wick contribution to effluent solute concentration (calculated by subtracting influent from effluent values) was highest for Na (90%, Fig. 7). Although wick contribution to effluent Si and Mg was lower, it was still substantial and showed large variation between replicates as indicated by large error bars. Negative wick contribution for Ca indicates uptake (rather than release) by the wicks.

DISCUSSION

Impact of Wicks on Soil Solution Chemistry

Any differences between influent and effluent solute concentration and speciation during the flow-through wick column experiment are a consequence of solution contact with the glass fiber wicks. Changes in solute concentration can result from (i) wick dissolution (increase in solute concentration) or (ii) adsorption (including uptake during ion exchange) or precipitation at the wick surface (decrease in solute concentration).

Dissolution of the glass fiber wicks is indicated by higher effluent than influent values for main glass constituents (Table 1). Most manufactured glasses are composed of SiO₂ (~60–80%), CaO, MgO, Al₂O₃, and other additions, such as B₂O₃ or F⁻, to improve durability (De Jong et al., 2000). With the exception of Al, all wick derived cations and F⁻ concentrations were higher in the effluent than the influent for both ASE and water. The fact that effluent DIC concentrations also increased (Fig. 2b) suggest that soda (Na₂CO₃) may also be present in the glass, since it is an addition typically made to facilitate glass processing (De Jong et al., 2000), although an increase in HCO₃⁻ is also expected to result simply from the increase in pH that was observed, assuming equilibrium with atmospheric CO₂. Wick reaction with the aqueous phase is in agreement with observations made by Goynes et al. (2000) who attributed to wick dissolution the higher alkalinity values and base cation concentration in fiberglass containing samplers compared to fiberglass free zero-tension samplers.

In addition to congruent dissolution, sorption, and cation exchange can also alter solution concentrations. In particular, the Group 1A and 2A metals K, Sr, and Ba showed lower effluent than influent concentrations. While Si is the glass forming element in the polymer network, other cations (and

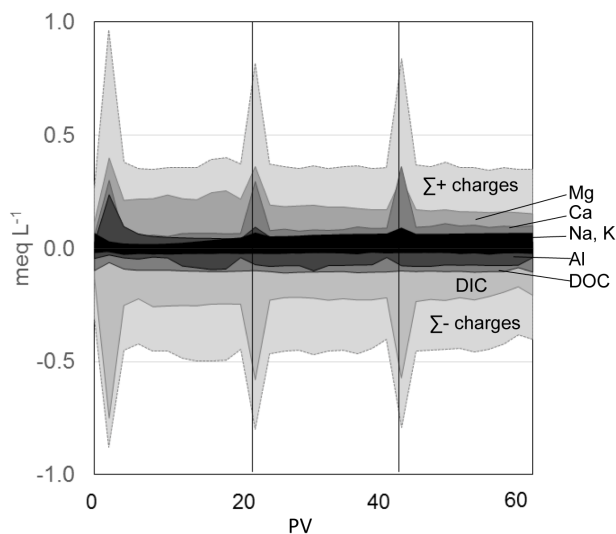


Fig. 6. Ion charge balance for influent (values at 0 PV) and effluent solutions over the course of the experiment. Dashed lines indicate the sum of negative and positive charges. Vertical lines indicate 24 h of stop flow.

anions such as F^- are typically network modifiers that are not structurally bound (Biscoe and Warren, 1938). Hence cation and anion exchange in the glass network structure, as well as on charged silanol sites, is a likely explanation for loss of K, Sr and Ba from ASE solution. The selective extraction of cations and B during the initial stage of glass dissolution was indeed shown in simulations by Devreux et al. (2001) and precede the overall congruent dissolution of the glass. Another explanation for the decreased concentrations of K, Sr, and Ba in the effluent is that these cations may be associated with colloidal material (e.g., adsorbed in interlayers of clay minerals) that occur in the ASE ($<0.45 \mu\text{m}$) filtrate solutions and that may adhere to the wick surface. Previous research has shown that clay mineral colloids can be retained at the wick water interface by physicochemical attachment (Czigány et al., 2005; Shira et al., 2006).

Concentrations of numerous solutes remained unaffected by passage over the fiberglass wicks. For these solutes sorption and/or wick dissolution were undetectable (Al, Mn, V, Fe, Co, Pb, U, and all REE+Y, Table 1 and 2). One subgroup of these solutes (Mn, Fe, Co, and Pb) showed a slight negative pulse in concentration after (re)-application of flow (Fig. 4f). In a previous study, Perdrial et al. (2012) showed a similar negative pulse for molar absorptivity (i.e., $SUVA_{254}$) values of DOM that was interpreted as a short-term preferential sorption of more aromatic DOM within the wicks. Metals that showed this negative pulse are known to form stable DOM complexes (Alloway, 1995), and could be retained as complexes at the water-wick interface.

Besides impacting soil solution concentration, solution-wick interaction also changes solute speciation, especially of DIC and Al (Table 3), primarily because of the increase in pH (Fig. 1a). A similar pH increase was

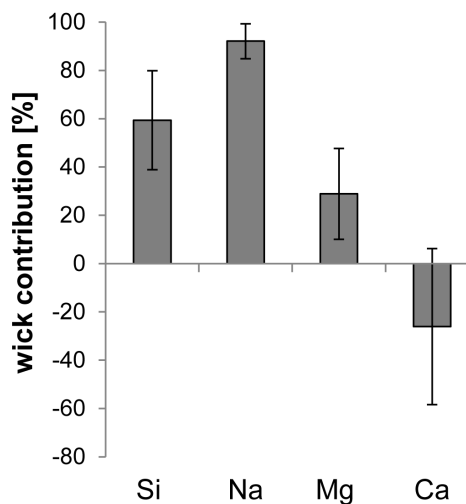


Fig. 7. Relative contribution of wick derived solutes determined at the full PCap scale.

observed in the study of Goyne et al. (2000) where pH of samples from glass fiber free ZTS were two to three pH units lower (pH 4) than that of the samples collected by PCaps (pH 6 and 7). In that study of an acid forest soil, Al was almost exclusively complexed with DOM at pH 4, but was calculated to be present as Al-hydroxide species at near neutral pH ($\sim 50\%$). In the present study, wick effects on Al speciation were less substantial because the pH of the influent solution was already near neutral (Table 3). These results suggest that each field site has to be evaluated with respect to its sensitivity toward pH changes and corresponding changes in speciation and metal-DOM complexation. Overall our results, combined with that of Goyne et al. (2000) suggest that fiberglass PCaps are more suitable for sampling near neutral pH soil solution.

Implications for the Suitability of Fiberglass Wick PCaps for Solute Flux Determination

Many of the tested elements were not affected by the presence of fiberglass wicks (see Table 4). With the caveat that soil physical effects of vadose zone sampling must be considered (Perdrial et al., 2012; Weihermüller, 2007), effluent elemental concentration for these elements can be assumed to accurately represent concentrations in mobile soil solutions (Table 1 and 2). However, the experimental results presented in this study clearly show that fiberglass wicks can introduce chemical artifacts, altering the composition of soil solution samples and cannot be used for determination of all inorganic solute fluxes without prior careful assessment, especially due to dissolution of the wick material that introduces Si and cationic metals (Table 4).

The full-scale experiment confirmed the pattern of wick dissolution leading to increases in glass constituents and

Table 4. Summary of impact of wicks on solutes:

Species	Not/moderately affected by wicks	Retained by wicks	Released by wicks
Major cations	–	Pt, K ⁺	B, Na, Mg, Si, Pt, K ⁺ , Ca
Anions	Cl ⁻ , NO ₃ ⁻ , SO ₄ ²⁻	–	F ⁻ ,
Trace metals	Al, Ti, Mn, V, Fe, Co, As, Y, Mo, Sn, Pb, U, REE	Cu, Sr	Cr, Sb

+Solute that are both retained and released by wicks

revealed that fractional contribution of wick derived solutes is especially high for Si (39–79%) and Na (85–99%, Fig. 7). In contrast, Ca was not released but rather retained by the wicks. This observation differs from the column experiment and could indicate cation exchange or precipitation that occurs only in the full scale experiment. Although all wicks wet up when solution infiltrates, not all of them are completely saturated or act as conductors for soil solution to the same extent. Hence, solutions surrounding individual wick fibers could become saturated with respect to, for example, $\text{CaCO}_3(s)$ that could then precipitate. Based on these results it is not recommended that fiberglass based PCap samples be used to elucidate weathering fluxes for solutes whose concentrations are altered by contact with the wicks.

CONCLUSIONS

The presence of fiberglass wicks, an integral part of the PCap sampling system, does not impact the concentration of many solutes in soil solution samples and PCaps can be used for solute flux determination for most anions and many trace metals. However, slow dissolution of wicks, cation exchange and/or colloidal retention alters the sample composition specifically with respect to major cation concentrations. The extent of release of wick constituents (Si, Na, Mg, and Ca) tested at full scale indicates that the signal of the sampled solution is swamped by dissolving wick material. Additionally, wick dissolution leads to an increase in pH that needs to be taken into account, particularly if solution phase data are to be used in aqueous geochemical modeling.

ACKNOWLEDGMENTS

The Jemez-Santa Catalina Critical Zone Observatory is supported by the National Science Foundation, Grant no. EAR-0724958. We thank Mary Kay Amistadi, Scott Compton, Tim Corley, Adrian Harpold, Mercer Meding, Alisson Peterson, and Craig Rasmussen for input and assistance with sampling and analysis. We also thank two anonymous reviewers and the AE Samira Daroub for thoughtful comments and suggestions.

REFERENCES

Alloway, B.J. 1995. Heavy metals in soils. In: B.J. Alloway, editor, Heavy metals in soils. Blackie Academic and Professional, London. p 368

Amiotte Suchet, P., J.-L. Probst, and W. Ludwig. 2003. Worldwide distribution of continental rock lithology: Implications for the atmospheric/soil CO_2 uptake by continental weathering and alkalinity river transport to the oceans. *Global Biogeochem. Cycles* 17:1038.

Barber, S.A. 1995. Soil nutrient bioavailability: A mechanistic approach. John Wiley & Sons, New York.

Biddle, D.L., D.J. Chittleborough, and R.W. Fitzpatrick. 1995. Field monitoring of solute and colloid mobility in a gneissic sub-catchment, South Australia. *Appl. Clay Sci.* 9:433–442. doi:10.1016/0169-1317(94)00035-O

Biscoe, J., and B.E. Warren. 1938. X-ray diffraction study of soda-boric oxide glass. *J. Am. Ceram. Soc.* 21:287–293. doi:10.1111/j.1151-2916.1938.tb15777.x

Boulding, J.R., and J.S. Ginn. 2004. Practical handbook of soil, vadose zone, and ground-water contamination. Assessment, prevention and remediation. CRC Press LLC, Boca Raton, FL.

Brandi-Dohrn, F.M., M. Hess, J.S. Selker, and R.P. Dick. 1996. Field evaluation of passive capillary samplers. *Soil Sci. Soc. Am. J.* 60:1705–1713. doi:10.2136/sssaj1996.03615995006000060014x

Chorover, J., P. Troch, C. Rasmussen, P.D. Brooks, J.D. Pelletier, D.D. Breshears,

T.E. Huxman, S. Papuga, K. Lohse, J.C. McIntosh, T. Meixner, M. Schaap, M.E. Litvak, J.N. Perdrial, A. Harpold, and A. Durcik. 2011. Probing how water, carbon, and energy drive landscape evolution and surface water dynamics: The Jemez River Basin–Santa Catalina Mountains Critical Zone Observatory. *Vadose Zone J.* 10:884–899. doi:10.2136/vzj2010.0132

Czigány, S., M. Flury, J.B. Harsh, B.C. Williams, and J.M. Shira. 2005. Suitability of fiberglass wicks to sample colloids from vadose zone pore water. *Vadose Zone J.* 4:175–183. doi:10.2113/4.1.175

De Jong, B.H.W.S., R.G.C. Beerkens, P.A. van Nijnatten, and E. Le Bourhis. 2000. Glass, 1. Fundamentals. In: Ullmann's encyclopedia of industrial chemistry. Wiley-VCH Verlag, Hoboken, NJ.

Devreux, F., P. Barboux, M. Filoche, and B. Sapoval. 2001. A simplified model for glass dissolution in water. *J. Mater. Sci.* 36:1331–1341. doi:10.1023/A:1017591100985

Felmy, A., D. Girvin, and E. Jenne. 1984. MINTEQA—A computer program for calculating aqueous geochemical equilibria. EPA/600/3-84/032, revised 2004. United States Environmental Protection Agency, Washington, DC.

Frisbee, M.D., F.M. Phillips, A.R. Campbell, and J.M.H. Hendrickx. 2010. Modified passive capillary samplers for collecting samples of snowmelt infiltration for stable isotope analysis in remote, seasonally inaccessible watersheds 1: Laboratory evaluation. *Hydrol. Processes* 24:825–833. doi:10.1002/hyp.7523

Goyné, K.W., R.L. Day, and J. Chorover. 2000. Artifacts caused by the collection of soil solution with passive capillary samplers. *Soil Sci. Soc. Am. J.* 64:1330–1336. doi:10.2136/sssaj2000.6441330x

Holder, M., K.W. Brown, J.C. Thomas, D. Zabcik, and H.E. Murray. 1991. Capillary-wick unsaturated zone soil pore water sampler. *Soil Sci. Soc. Am. J.* 55:1195–1202. doi:10.2136/sssaj1991.03615995005500050001x

Ilg, K., E. Ferber, H. Stoffregen, A. Winkler, A. Pekdeger, M. Kaupenjohann, and J. Siemens. 2007. Comparing unsaturated colloid transport through columns with differing sampling systems. *Soil Sci. Soc. Am. J.* 71:298–305. doi:10.2136/sssaj2006.0145

Jabro, J.D., Y. Kim, R.G. Evans, W.M. Iversen, and W.B. Stevens. 2008. Passive capillary sampler for measuring soil water drainage and flux in the vadose zone: Design, performance, and enhancement. *Appl. Eng. Agric.* 24:439–446. doi:10.13031/2013.25145

Knutson, J.H., S.B. Lee, W.Q. Zhang, and J.S. Selker. 1993. Fiberglass wick preparation for use in passive capillary wick soil pore-water samplers. *Soil Sci. Soc. Am. J.* 57:1474–1476.

Louie, M.J., P.M. Shelby, J.S. Smerud, L.O. Gatchell, J.S. Selker, and R.M. Shelby. 2000. Field evaluation of passive capillary samplers for estimating groundwater recharge. *Water Resour. Res.* 36:2407–2416. doi:10.1029/2000WR900135

Mertens, J., J. Diels, J. Feyen, and J. Vanderborght. 2007. Numerical analysis of passive capillary wick samplers prior to field installation. *Soil Sci. Soc. Am. J.* 71:35–42. doi:10.2136/sssaj2006.0106

Miro, M., W.J. Fitz, S. Swoboda, and W.W. Wenzel. 2010. In-situ sampling of soil pore water: Evaluation of linear-type microdialysis probes and suction cups at varied moisture contents. *Environ. Chem.* 7:123–131. doi:10.1071/EN09084

Perdrial, J.N., N. Perdrial, A. Harpold, X. Gao, K.M. LaSharr, and J. Chorover. 2012. Impacts of sampling dissolved organic matter with passive capillary wicks versus aqueous soil extraction. *Soil Sci. Soc. Am. J.* 76:2019–2030. doi:10.2136/sssaj2012.0061

Peters, A., and W. Durner. 2009. Large zero-tension plate lysimeters for soil water and solute collection in undisturbed soils. *Hydrol. Earth Syst. Sci.* 13:1671–1683. doi:10.5194/hess-13-1671-2009

Shira, J.M., B.C. Williams, M. Flury, S. Czigany, and M. Tuller. 2006. Sampling silica and ferrihydrite colloids with fiberglass wicks under unsaturated conditions. *J. Environ. Qual.* 35:1127–1134. doi:10.2134/jeq2005.0136

Soil Survey Staff. 2010. Keys to soil taxonomy. United States Department of Agriculture–NRCS, Washington, DC.

Townshend A., C. Poole, and P. Worsfold, editors. 2005. GLASSES. In: Encyclopedia of analytical science. (2nd ed.). Elsevier, Oxford. p. 208–214

Weihermüller, L., J. Siemens, M. Deurer, S. Knoblauch, H. Rupp, A. Goettlein, and T. Puetz. 2007. In situ soil water extraction: A review. *J. Environ. Qual.* 36:1735–1748. doi:10.2134/jeq2007.0218

Zhu, Y., R.H. Fox, and J.D. Toth. 2002. Leachate collection efficiency of zero-tension pan and passive capillary fiberglass wick lysimeters. *Soil Sci. Soc. Am. J.* 66:37–43. doi:10.2136/sssaj2002.0037